JOURNAL OF CIVIL ENGINEERING AND MANAGEMENT
ISSN 1392-3730 print/ISSN 1822-3605 online
2013 Volume 19(4): 476–491
doi:10.3846/13923730.2013.768546

NON-LINEAR DYNAMIC ANALYSIS OF COUPLED SPAR PLATFORM

Mohammed JAMEEL[a,b], Suhail AHMAD[a,b], A. B. M. Saiful ISLAM[a,b], Mohd Zamin JUMAAT[a,b]

[a]*Department of Civil Engineering, University of Malaya, Kuala Lumpur, Malaysia*
[b]*Department of Applied Mechanics, Indian Institute of Technology Delhi, India*

Received 12 Aug. 2011; accepted 4 Nov. 2011

Abstract. Spar platforms are treated as cost-effective and resourceful type of offshore structure in deep water. With increasing depth there are significant changes in its structural behaviour due to coupling of spar hull-mooring line along with radical influence of mooring line damping. So these phenomena should be precisely counted for accurate motion analysis of spar mooring system. In present study, spar platform are configured as a single fully coupled integrated model in ABAQUS/AQUA. Non-linear dynamic analysis in time domain is performed adopting Newmark-β automatic time incrementation technique. Non-linearities due to geometric, loading and boundary conditions are duly considered. Displacement and rotational responses of spar and mooring tensions are obtained during long-duration storm. spar responses get significantly modified and mean position of oscillations gets shifted after longer wave loading. The surge, heave and pitch responses are predominantly excited respectively. The energy contents of PSDs of these responses reduce considerably after long wave loading. Mooring tension responses are significantly different reflecting the damping effect of mooring lines. The pitch response is fairly sensitive to the wave loading duration. After long duration of storm the wave frequency response increases. However, low frequency and wave frequency responses may simultaneously occur due to synchronising sea states.

Keywords: offshore structure; spar platform; integrated coupled; non-linear dynamic; catenary mooring; long durational storm.

Reference to this paper should be made as follows: Jameel, M.; Ahmad, S.; Islam, A. B. M. S.; Jumaat, M. Z. 2013. Non-linear dynamic analysis of coupled spar platform, *Journal of Civil Engineering and Management* 19(4): 476–491. http://dx.doi.org/10.3846/13923730.2013.768546

Introduction

Exploration and development of offshore oil and gas in shallow and intermediate water depths has traditionally been carried out using the conventional jacket type fixed platforms. As the water depth increases fixed platforms become expensive and uneconomical. The prominence afterwards shifts to floating production systems (Hillis, Courtney 2011; Islam *et al.* 2012; Jameel *et al.* 2011). Spar platform is such a compliant floating structure used for deepwater applications of drilling, production, processing and storage plus offloading of ocean deposits (Halkyard 1996). Numerous studies have recently been performed in order to assess the effect of the coupling on different offshore floating production systems/spar buoy (Chen *et al.* 2001; Colby *et al.* 2000; Culla, Carcaterra 2007; Gupta *et al.* 2000; Ormberg, Larsen 1998; Ran, Kim 1997; Ran *et al.* 1996). Coupled dynamic behaviours of hull/mooring/riser elements of spar platform have correspondingly been investigated by some other researchers (Chen *et al.* 2006; Jameel, Ahmad 2011; Kim *et al.* 2001a, b, 2005). Ma and Patel (2001) have conducted parametric studies on spar and TLP for different depths for deep water. Chen and Zhang (1999) presented the response of a spar constrained by slack mooring lines to steep ocean waves by two different schemes: a quasi-static approach (SMACOS), and a coupled dynamic approach (COUPLE) to reveal the coupling effects between a spar and its mooring system. In coupled dynamic approach, dynamics of the mooring system are calculated using a numerical programme, known as CABLE3D. Ran *et al.* (1999) studied coupled dynamic analysis of a moored spar in random waves and currents. They followed the solution in time-domain and frequency-domain analysis. In the recent days of advancement, non-linear dynamic response analysis of spar and similar structures has been carried out by a few scholars (Grigorenko, Yaremchenko 2009; Islam *et al.* 2011a; Kim, Lee 2011; Noorzaei *et al.* 2010). Umar and Datta (2003)

Corresponding author: A. B. M. Saiful Islam
E-mail: abm.saiful@gmail.com

Taylor & Francis
Taylor & Francis Group

have shown the non-linear response conduct of a moored buoy. The wave induced excursions in different directions of spars (Luo, Zhu 2006; Mei 2009; Sarkar, Roesset 2004; Shah *et al.* 2005; Srinivasan *et al.* 2008; Yang, Kim 2010) are well surveyed.

Some researchers investigated the coupling effect of the spar mooring system (Chaudhury 2001; Chaudhury, Ho 2000; Ding *et al.* 2003, 2005; Garrett 2005; Koo *et al.* 2004; Vazquez-Hernandez *et al.* 2006). Tahar and Kim (2008) developed numerical tool for coupled analysis of deepwater floating platform with polyester mooring lines. Low and Langley (2008) presented a hybrid time/frequency-domain approach for coupled analysis of vessel/mooring/riser. The vessel was modelled as a rigid body with six degrees of freedom, and the lines were discretized as lumped masses connected by linear extensional and rotational springs. The method was found to be in good agreement with fully coupled time-domain analysis, when used for relatively shallow water depths. Low (2008) used the same hybrid method to predict the extreme responses of coupled floating structure. Zhang *et al.* (2008) studied the effect of coupling for cell-truss spar platform. The spar mooring/riser was modelled by three methods namely quasi-static coupled, semi-coupled and coupled. The results from frequency-domain and time-domain analyses were compared with experimental data. Yang and Kim (2010) carried out coupled analysis of hull-tendon-riser for a TLP. The mooring line/riser/tendon system was modelled as elastic rod. It was connected to the hull by linear and rotational springs. The equilibrium equations of hull and mooring line/risers/tendon system were solved simultaneously. Yung *et al.* (2004) presented the advancement of Spar VIV Prediction. Ma *et al.* (2009) reported feed forward and feedback optimal control with memory for offshore platforms under irregular wave forces. In addition, coupled effects of risers/supporting guide frames on spar responses were explored by Zhang and Zou (2002) and spar mooring system by Islam *et al.* (2011b).

In the existing analysis methods, force and displacement of mooring heads and vessel fairleads are iteratively matched at every instant of time-marching scheme, while solving the equilibrium equations. However, the velocity and acceleration do not reportedly match. Further, the continuity of vessel and mooring is missing. In this process the major contribution of moorings in terms of drag, inertia and damping due to their longer lengths, larger sizes and heavier weights are not fully incorporated. This effect is more pronounced in deepwater conditions. Furthermore, the behaviour after a long period of wave hitting has not been assessed. Hence, the main objective of present study is to idealise the spar mooring integrated system as a fully/strongly coupled system, to introduce a new mathematical approach for solution of coupled spar mooring system, as well as to study the damping effects on mooring lines and the importance of coupling effect on spar platform.

The fully coupled integrated spar mooring line system has been implemented in this research. This essentially means that the spar hull is physically linked with mooring lines at fairleads provided by six non-linear springs. The spar hull has been modelled as large cylinder (Rasiulis, Gurkšnys 2010). The mooring lines, as an integral part of the system support the spar at fairlead and pinned at the far end on the seabed (Fig. 1). They partly hang and partly lie on the sea bed. Sea bed is modelled as a large flat surface with a provision to simulate mooring contact behaviour. The mooring line dynamics takes into account the instantaneous tension fluctuation and damping forces with time-wise variation of other properties. These forces are active concurrently on spar hull cylinder. Hence, it is not needed to match the force, displacement, velocity and acceleration at the fairlead location iteratively. The output from such analyses is horizontal, vertical and rotational motions of platform and mooring line responses. Finite element code ABAQUS/AQUA (ABAQUS 2006) is found to be suitable for the present study. Modelled spar mooring system has been analysed in effect of proper environmental loading at regular wave. The structural response behaviour in steady state after 2000 and 8000 sec. of wave hitting have been extracted in the form of surge, heave and pitch motion.

1. Mathematical formulation

The formation of a non-linear deterministic model for coupled dynamic analysis includes the formulation of a non-linear stiffness matrix, allowing for mooring line tension fluctuations subjected to variable buoyancy, as well as structural and environmental non-linearities. The model involves selection and solution of wave theory that reasonably represents the water particle kinematics to estimate the drag and inertia for all the six degrees of freedom. The static coupled problem is solved by Newton's method. In order to incorporate high degrees of non-linearities, an iterative time-domain numerical integration is required to solve the equation of motion and to obtain the response time histories. The Newmark-β

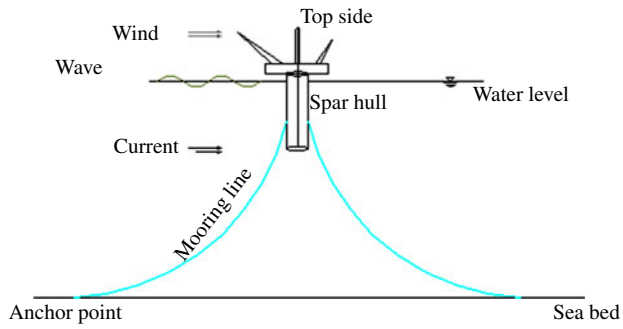

Fig. 1. Spar mooring system

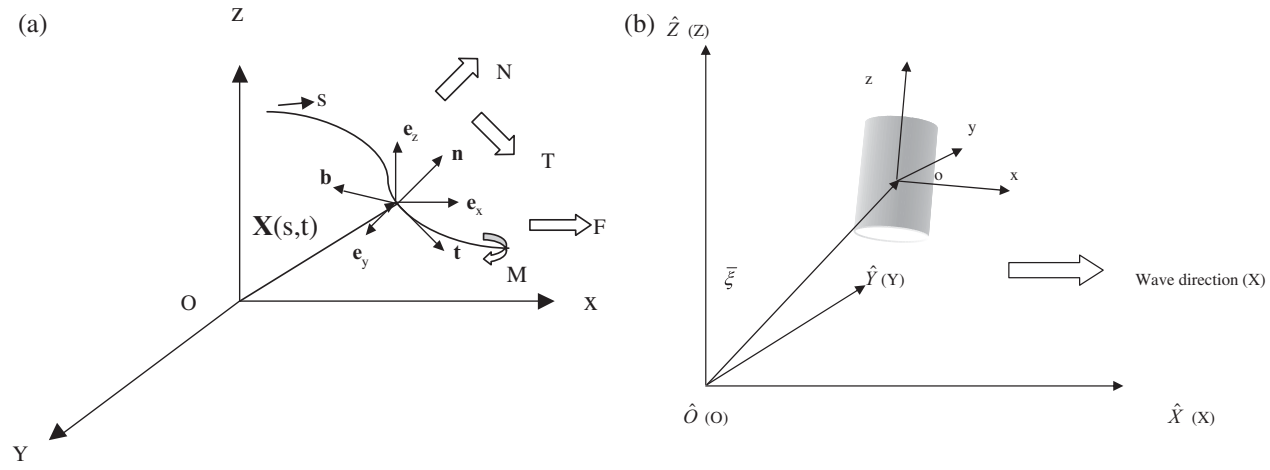

Fig. 2. Coordinate system (a) of mooring line and (b) for rigid spar hull

time integration scheme with iterative convergence has been adopted for solving the coupled dynamic model. Following assumptions are made to model the complex spar mooring structure in deep-sea loading:

- The mooring line is modelled as hybrid beam element;
- The spar hull is rigid cylinder;
- Mooring line is attached by springs at fairlead of spar hull with hinge connection. The other end of mooring is anchored to sea bed. There is no friction between mooring and sea bed;
- Airy's wave theory is adopted to calculate the water particle kinematics;
- The Morison's equation is sufficient to calculate the wave exiting forces;
- The distortion of waves by spar and mooring lines is insignificant.

Table 1. Mechanical and geometrical properties of spar and moorings

Parameter		Magnitude
Water depth		1018 m
Spar (classic JIP spar)	Length	213.044 m
	Diameter	40.54 m
	Draft	198.12 m
	Mass	2.515276E+08 kg
	Mooring point	106.62 m
	Number of nodes	17
	Number of elements	16
	Type of element	Rigid beam element
Mooring	Number of moorings	4
	Stiffness (EA)	1.50E+09 N
	Length	2000.0 m
	Mass	1100 kg/m
	Mooring line pretension	1.625E+07 N
	No. of nodes	101
	Element type	Hybrid beam element

The equation of motion for spar mooring system is as follows:

$$[M]\{\ddot{X}\} + [C]\{\dot{X}\} + [K]\{X\} = \{F(t)\}, \qquad (1)$$

where $\{X\}$ – 6 DOF structural displacements at each node, $\{\dot{X}\}$ – structural velocity vector, $\{\ddot{X}\}$ – structural acceleration vector, $[M]$ – total mass matrix $= [M]^{Spar+\ Mooring\ lines} + [M]^{Added\ mass}$; [C] – damping matrix $= [C]^{Structural\ damping} + [C]^{Hydrodynamic\ damping}$, $[K]$ – stiffness matrix $= [K]^{Elastic} + [K]^{Geometric}$.

Total forces on the spar mooring system are denoted by $\{F(t)\}$. The dot symbolises differentiation with respect to time. The total spar mooring mass matrix of the system consists of structural mass and added mass components. The structural mass of the spar mooring system is made up of elemental consistent mass matrices of the moorings and lumped mass properties of the rigid spar hull. The lumped mass properties are assumed to be concentrated at the CG of spar hull. The added mass of the structure occurs due to the water surrounding the entire structure. Considering the oscillation of the free surface, this effect of variable submergence is simulated as per Wheeler's approach.

The total stiffness matrix element $[K]$ consists of two parts, the elastic stiffness matrix $[K_E]$ and the

Table 2. Hydrodynamic properties

Element	Coefficient
Spar hull	Drag coefficient: 0.6 Inertia coefficient: 2.0 Added mass coefficient: 1.0
Mooring line	Drag coefficient: 1.0 Inertia coefficient: 2.2 Added mass coefficient: 1.2

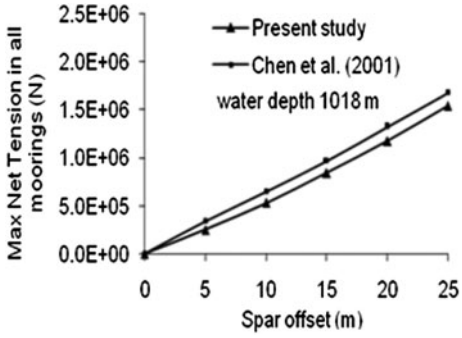

Fig. 3. Tension comparison for 1018 m water depth

geometrical stiffness matrix [K_G]. The overall damping to the system is being offered by structural, as well as hydrodynamic damping. The major damping is induced due to the hydrodynamic effects. It may be obtained if the structure velocity term in the Morison equation is transferred from the force vector on right hand side to the damping term on the left hand side in the governing equation of motion. The structural damping is simulated by Rayleigh damping. It follows Eqn (2) in which ξ signifies structural damping ratio, Φ is modal matrix, ω_i denotes natural frequency and m_i implies the generalised mass:

$$\Phi^T[C]^{Structural}\Phi = [2\xi\omega_i m_i]. \quad (2)$$

1.1. Idealisation for catenary mooring

In a 3-D Cartesian coordinate system, the configuration of a mooring line is expressed in terms of a vector, $\vec{X}(s,t)$, which is a function of s, the deformed arc length along the rod, and time t. In Figure 2a, t, n and b are unit vectors in tangential, normal and bi-normal directions correspondingly, and e_x, e_y and e_z are unit vectors in X-, Y- and Z-axes, respectively. The internal state of stress at a point on the mooring line is described fully by the resultant force N and the resultant moment M acting at the centreline of the rod.

The external forces applied on a catenary mooring line involve the gravity forces, hydrostatic forces and hydrodynamic forces. The wave force $F(X, Z, t)$ per unit length of mooring line acting on a single mooring line of diameter D_m can be derived as follows:

$$F(X,Z,t) = F_{Gravity} + F_{Inertia} + F_{Drag} + F_{Seawater}^{F-K}, \quad (3)$$

Table 3. Comparison of natural time periods

	Time periods (sec.)	
	Chen *et al.* (2001)	Present study
Surge	331.86	341.97
Heave	29.03	22.60
Pitch	66.77	43.48

which implies that:

$$\begin{aligned} F = {} & (\rho_w A_m - \rho_i A_i - \rho_t A_t) g e_z + \\ & \rho_w A_m (I + C_{Mn} N + C_{Mt} T)(\ddot{u} - \ddot{X}) + \\ & \frac{1}{2}\rho_w D C_{Dn} N(\dot{u} - \dot{X})\left|N(\dot{u} - \dot{X})\right| + \\ & \frac{1}{2}\rho_w D C_{Dt} T(\dot{u} - \dot{X})\left|T(\dot{u} - \dot{X})\right|, \end{aligned} \quad (4)$$

The values of the velocity $\dot{u}$ and acceleration $\ddot{u}$ in Eqn (4) are calculated from an appropriate wave theory. In the above equations, prime indicates that the derivative is being done with respect to the arc length s of mooring line. C_D symbolises as drag coefficient and C_M as inertia coefficient. The subscripts n and t indicate normal and tangential direction of Cartesian coordinate system of mooring line respectively. Other symbols are denoted as follows: $\rho_m = \rho_t A_t + \rho_i A_i$, the mass per unit mooring line; ρ_w, the mass density of the sea water, ρ_i, the mass density of the inside fluid; ρ_t, the mass density of the tube; A_m, the outer cross-section area of the mooring line; D_m, the diameter of mooring line; A_i, the inner cross-section area of the mooring line; A_t, the structural cross-section area of the mooring line; P_w, pressure of the sea water; P_i, pressure of the internal fluid; N, T, transfer matrices of normal and tangential forces; I, identity matrix.

The subscripts w, i and t denote the sea water, the fluid inside the tube and the tube itself. T and N are defined by $T = X'^T X'$ and $N = I - T$. As the motion of the structure is considered, there will be addition of some force exerted per unit to length acting due to structural acceleration of a mooring line element equivalent to $\rho_w A_m \mathrm{X}$. Taking into account the foregoing

Table 4. Statistical response of spar mooring system after 2000 sec. of wave hitting

Dynamic responses	+ve peak	−ve peak	Standard deviation	Mean
Surge (m)	16.461	−14.105	9.196	1.043
Heave (m)	2.453	−2.098	1.217	0.389
Pitch (rad.)	0.203	−0.135	0.079	0.0001
Tension in mooring line 1 (N)	1.6821E+07	1.5924E+07	2.6436E+05	1.6395E+7
Tension in mooring line 3 (N)	1.6804E+07	1.5743E+07	2.5037E+05	1.6298E+07

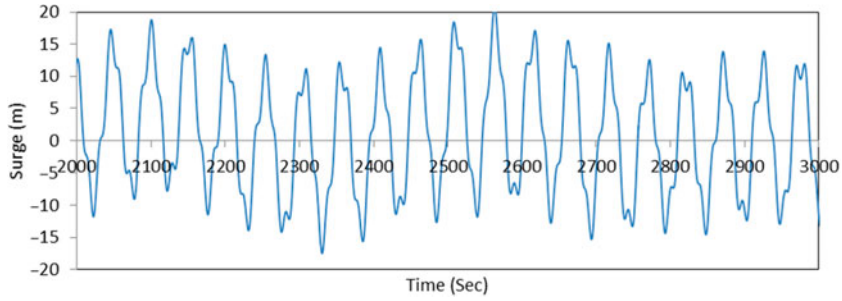

Fig. 4. Surge time series after 2000 sec. of wave hitting

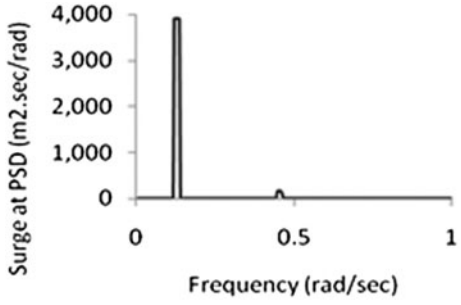

Fig. 5. Surge response at PSD after 2000 sec. of wave hitting

modification, that is, adding this term in Eqn (4), the total force acting on mooring line comes up as:

$$F = (\rho_w A_m - \rho_i A_i - \rho_t A_t) g e_z + \rho_w A_m (I + C_{Mn} N + C_{Mt} T)\ddot{u} - \rho_w (C_m - 1) A_m \ddot{X} + \frac{1}{2}\rho_w D C_{Dn} N(\dot{u} - \dot{X})\left|N(\dot{u} - \dot{X})\right| + \frac{1}{2}\rho_w D C_{Dt} T(\dot{u} - \dot{X})\left|T(\dot{u} - \dot{X})\right|. \quad (5)$$

The virtual mass matrix is simplified as:

$$[M]^{Mooring} = (\rho_t A_t + \rho_i A_i) I + \rho_w A_m C_{Mn} N + \rho_w A_m C_{Mt} T. \quad (6)$$

Considering the current velocity, u_c along with wave velocity Eqn (5) is modified as:

$$\{F(t)\} = (\rho_w A_m - \rho_i A_i - \rho_t A_t) g e_z + \rho_w A_m (I + C_{Mn} N + C_{Mt} T)\ddot{u} - \rho_w (C_m - 1) A_m \ddot{X} + \frac{1}{2}\rho_w D_m C_{Dn} N(\dot{u} + u_c - \dot{X})\left|N(\dot{u} + u_c - \dot{X})\right| + \frac{1}{2}\rho_w D_m C_{Dt} T(\dot{u} + u_c - \dot{X})\left|T(\dot{u} + u_c - \dot{X})\right|. \quad (7)$$

Hence, the dynamic equilibrium equation of mooring line can be obtained as:

$$[M]^{Mooring}\{\ddot{X}\} + \left(\frac{[2\xi\omega_{im} m_{im}]}{\Phi^T \Phi} + [C]^{hydrodynamic}\right)\{\dot{X}\} + \left([K]_E^{Mooring} + [K]_G^{Mooring}\right)\{X\} = (\rho_w A_m - \rho_i A_i - \rho_t A_t) g e_z + \rho_w A_m (I + C_{Mn} N + C_{Mt} T)\ddot{u} - \rho_w (C_m - 1) A_m \ddot{X} + \frac{1}{2}\rho_w D_m C_{Dn} N(\dot{u} + u_c - \dot{X})\left|N(\dot{u} + u_c - \dot{X})\right| + \frac{1}{2}\rho_w D_m C_{Dt} T(\dot{u} + u_c - \dot{X})\left|T(\dot{u} + u_c - \dot{X})\right|. \quad (8)$$

1.2. Idealisation of rigid spar hull

Two coordinate systems are employed in the derivation of motion equations of a floating rigid body. Coordinate system $\hat{o}\hat{x}\hat{y}\hat{z}$ is a space-fixed coordinate system, while $oxyz$ is the body-fixed coordinate system moving with the body. The origin o can be the centre of gravity (g) or any point fixed on the body. The body-fixed coordinate $oxyz$ coincides with $\hat{o}\hat{x}\hat{y}\hat{z}$ when the body is at its initial position (Fig. 2b). A third coordinate system $OXYZ$ which is a spaced-fixed coordinate system with OXY plan lying on the free surface and Z-axis positive upwards is also introduced as a reference coordinate system. Incoming waves are given in this space-fixed reference coordinate system.

Therefore, the total force $F(X, Z, t)$ per unit length of spar hull cylinder of diameter D_s can be derived as follows:

$$F(X, Z, t) = F_{Gravity} + Fn_{Inertia} + Fn_{Drag} + F_{Axial} + F_{Lifting}, \quad (9)$$

Table 5. Statistical response of spar mooring system after 8000 sec. of wave hitting

Dynamic responses	+ve peak	−ve peak	Standard deviation	Mean
Surge (m)	8.143	−8.342	4.913	0.412
Heave (m)	1.433	−0.859	0.846	0.281
Pitch (radians)	0.072	−0.063	0.040	0.0000
Tension in mooring line 1 (N)	1.6695E+07	1.5834E+07	2.3835E+05	1.6329E+07
Tension in mooring line 3 (N)	1.6702E+07	1.5816E+07	2.3658E+05	1.6335+07

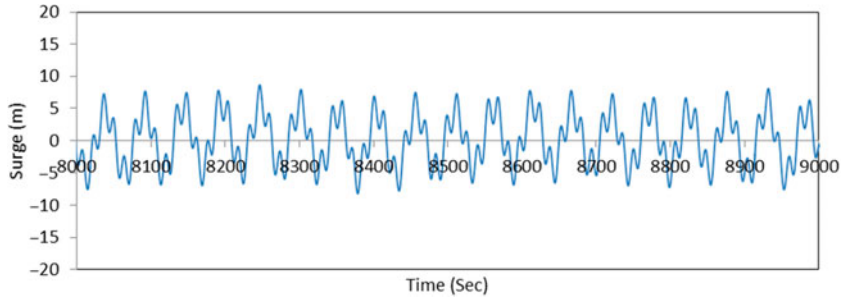

Fig. 6. Surge time series after 8000 sec. of wave hitting

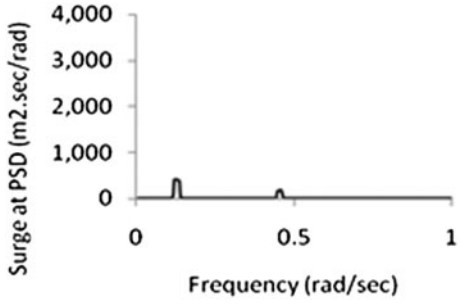

Fig. 7. Surge response at PSD after 8000 sec. of wave hitting

which implies that:

$$\begin{aligned} F = &- \rho_t g A_s e_z + \\ &\rho_w A_s C_M(\ddot{u}_n - \ddot{X}_n) + \\ &\rho_w A_s C_M \ddot{u}_n + \frac{1}{2}\rho_w D_s C_D(\dot{u}_n - \dot{X}_n)\left|(\dot{u}_n - \dot{X}_n)\right| + \\ &\frac{1}{2}\rho_w C_L D_s v_c^2 \cos(2\pi f \cdot t)\vec{e}_t \times \vec{e}_c + \\ &\rho_w \iint_{S_B}\left(\frac{\partial(\varphi^{(1)} + \varphi^{(2)}}{\partial t} + \frac{1}{2}\left|\nabla\varphi^{(1)}\right|^2\right)ds + \\ &C_{mt}\rho_w \frac{4}{3}\left(\frac{D_s}{2}\right)^3\left[\ddot{u}_t - \ddot{X}_t\right] + \\ &\frac{1}{2}\rho_w C_{Dt} A_s(\dot{u}_t - \dot{X}_t)\left[(\dot{u}_t - \dot{X}_t)\right], \end{aligned} \tag{10}$$

where ρ_s – the mass density of the spar, D_s – the diameter of the spar hull, A_s – the cross-section area of the spar hull; $\vec{e}_t$ – unit vectors in the axial direction, $\vec{e}_c$ – unit vectors in the current direction, C_L – the lifting coefficient, f – the vortex shedding frequency, S_o – Strouhal number, u_c – current velocity, $\varphi^{(1)}$ and $\varphi^{(2)}$ – the first- and second-order potential of incident waves.

Taking into account the added forces considering motion, foregoing modification of the total force acting on the spar hull comes up as:

$$\begin{aligned} F = &- \rho_t g A_s e_z + \\ &\rho_w A_s C_M(\ddot{u}_n - \ddot{X}_n) + \\ &\rho_w A_s C_M \ddot{u}_n + \frac{1}{2}\rho_w D_s C_D(\dot{u}_n - \dot{X}_n)\left|(\dot{u}_n - \dot{X}_n)\right| + \\ &\frac{1}{2}\rho_w C_L D_s v_c^2 \cos(2\pi f \cdot t)\vec{e}_t \times \vec{e}_c + \\ &\rho_w \iint_{S_B}\left(\frac{\partial(\varphi^{(1)} + \varphi^{(2)}}{\partial t} + \frac{1}{2}\right)\left|\nabla\varphi^{(1)}\right|^2 ds + \\ &C_{mt}\rho_w \frac{4}{3}\left(\frac{D_s}{2}\right)^3\left[\ddot{u}_t - \ddot{X}_t\right] + \\ &\frac{1}{2}\rho_w C_{Dt} A_s(\dot{u}_t - \dot{X}_t)\left[(\dot{u}_t - \dot{X}_t)\right] + \\ &\rho_w A_s \mathrm{X}_n. \end{aligned} \tag{11}$$

After including the effect of current the equation for spar hull leads to:

$$\begin{aligned} &[Ms + M_a s]\{\ddot{X}\} + \left(\frac{[2\xi\omega_{is}m_{is}]}{\Phi^T\Phi} + [C]^{hydrodynamic}\right)\{\dot{X}\} + \\ &\left([K]_E^{Spar} + [K]_G^{Spar}\right)\{X\} = \\ &\quad - \rho_t g A_s e_z + \\ &\quad \rho_w A_s C_M(\ddot{u}_n - \ddot{X}_n) + \end{aligned}$$

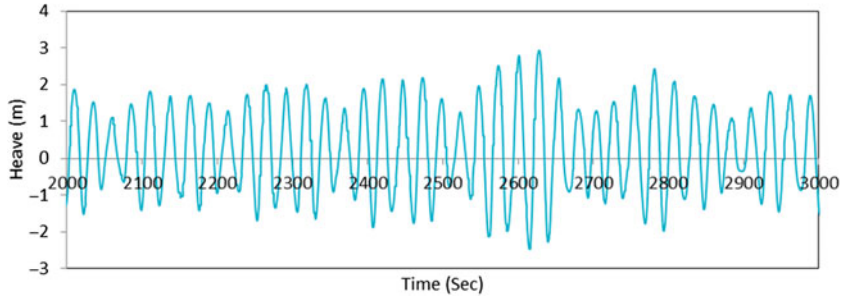

Fig. 8. Heave time series after 2000 sec. of wave hitting

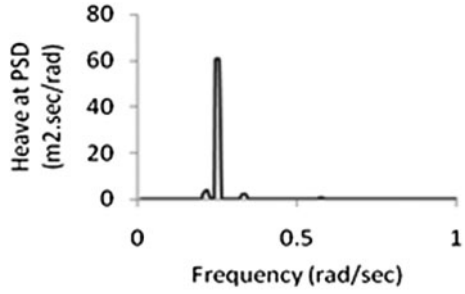

Fig. 9. Heave response at PSD after 2000 sec. of wave hitting

$$\rho_w A_s C_M \ddot{u}_n + \frac{1}{2}\rho_w D_s C_D(\dot{u}_n + u_c - \dot{X}_n)\left|(\dot{u}_n + u_c - \dot{X}_n)\right| + \frac{1}{2}\rho_w C_L D_s v_c^2 \cos(2\pi f.t)\vec{e}_t \times \vec{e}_c + \rho_w \iint_{S_B}\left(\frac{\partial(\varphi^{(1)}+\varphi^{(2)}}{\partial t} + \frac{1}{2}\left|\nabla\varphi^{(1)}\right|^2\right)ds + C_{mt}\rho_w \frac{4}{3}\left(\frac{D_s}{2}\right)^3\left[\ddot{u}_t - \ddot{X}_t\right] + \frac{1}{2}\rho_w C_{Dt} A_s(\dot{u}_t + u_c - \dot{X}_t)\left[(\dot{u}_t + u_c - \dot{X}_t)\right] + \rho_w A_s \mathrm{X}_n. \quad (12)$$

1.3. Equation of motion for spar platform

Formation of equation of motion for spar platform which combines spar hull and mooring lines in a single integrated system can be expressed as the following relation:

$$[M + M_a]^{Spar+Mooring}\{\ddot{X}\} + \left(\frac{[2\xi\omega_i m_i]}{\Phi^T\Phi} + [C]^{hydrodynamic}\right)\{\dot{X}\} + \left([K]_E^{Spar+Mooring} + [K]_G^{Spar+Mooring}\right)\{X\} = (\rho_w A_m - \rho_i A_i - \rho_t A_t)ge_z + \rho_w A_m(I + C_{Mn}N + C_{Mt}T)\ddot{u} - \rho_w(C_m - 1)A_m\ddot{X} + \frac{1}{2}\rho_w D_m C_{Dn} N(\dot{u} + u_c - \dot{X})\left|N(\dot{u} + u_c - \dot{X})\right| + \frac{1}{2}\rho_w D_m C_{Dt} T(\dot{u} + u_c - \dot{X})\left|T(\dot{u} + u_c - \dot{X})\right| - \rho_t g A_s e_z + \rho_w A_s C_M(\ddot{u}_n - \ddot{X}_n) + \rho_w A_s C_M \ddot{u}_n + \frac{1}{2}\rho_w D_s C_D(\dot{u}_n + u_c - \dot{X}_n)\left|(\dot{u}_n + u_c - \dot{X}_n)\right| + \frac{1}{2}\rho_w C_L D_s v_c^2 \cos(2\pi f.t)\vec{e}_t \times \vec{e}_c + \rho_w \times \iint_{S_B}\left(\frac{\partial(\varphi^{(1)}+\varphi^{(2)}}{\partial t} + \frac{1}{2}\left|\nabla\varphi^{(1)}\right|^2\right)ds + C_{mt}\rho_w\frac{4}{3} \times \left(\frac{D_s}{2}\right)^3\left[\ddot{u}_t - \ddot{X}_t\right] + \frac{1}{2}\rho_w C_{Dt}A_s(\dot{u}_t + u_c - \dot{X}_t) \times \left[(\dot{u}_t + u_c - \dot{X}_t)\right] + \rho_w A_s \mathrm{X}_n. \quad (13)$$

Therefore, after rearrangements, the motion equation of spar mooring system can be obtained as:

$$[M + M_a]^{Spar+Mooring}\{\ddot{X}\} + \left(\frac{[2\xi\omega_i m_i]}{\Phi^T\Phi} + [C]^{hydrodynamic}\right)\{\dot{X}\} + \left([K]_E^{Spar+Mooring} + [K]_G^{Spar+Mooring}\right)\{X\} = (\rho_w A_m - \rho_i A_i - \rho_t A_t)ge_z + \rho_w A_m(I + C_{Mn}N + C_{Mt}T)\ddot{u} - \rho_w(C_m - 1)A_m\ddot{X} + \frac{1}{2}\rho_w D_m C_{Dn} N(\dot{u} + u_c - \dot{X})\left|N(\dot{u} + u_c - \dot{X})\right| + \frac{1}{2}\rho_w D_m C_{Dt} T(\dot{u} + u_c - \dot{X})\left|T(\dot{u} + u_c - \dot{X})\right| - \rho_t g A_s e_z + \rho_w A_s(\ddot{X}_n + C_M(2\ddot{u}_n - \ddot{X}_n)) + \frac{1}{2}\rho_w D_s C_D(\dot{u}_n + u_c - \dot{X}_n)\left|(\dot{u}_n + u_c - \dot{X}_n)\right| + \frac{1}{2}\rho_w C_L D_s v_c^2 \cos(2\pi f \cdot t)\vec{e}_t \times \vec{e}_c + \rho_w \iint_{S_B}\left(\frac{\partial(\varphi^{(1)}+\varphi^{(2)}}{\partial t} + \frac{1}{2}\left|\nabla\varphi^{(1)}\right|^2\right)ds + C_{mt}\rho_w \frac{4}{3}\left(\frac{D_s}{2}\right)^3\left[\ddot{u}_t - \ddot{X}_t\right] + \frac{1}{2}\rho_w C_{Dt} A_s(\dot{u}_t + u_c - \dot{X}_t)\left[(\dot{u}_t + u_c - \dot{X}_t)\right].$$

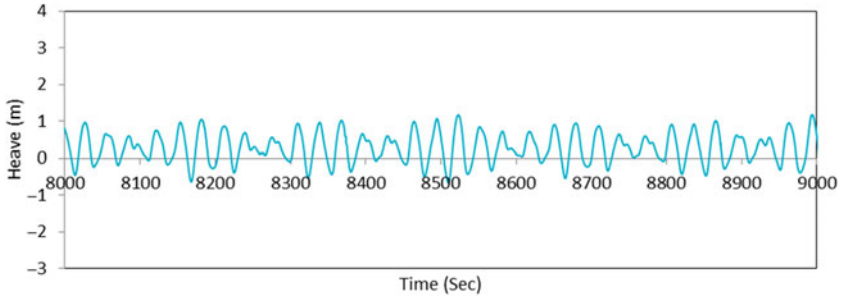

Fig. 10. Heave time series after 8000 sec. of wave hitting

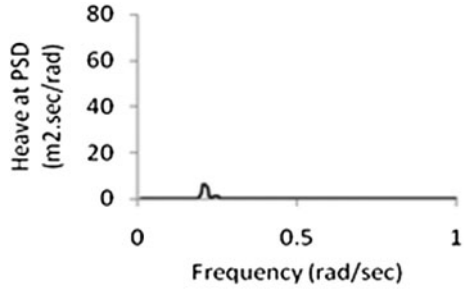

Fig. 11. Heave response at PSD after 8000 sec. of wave hitting

The analysis of spar platform considering actual physical coupling between the rigid vertical floating hull and mooring lines is possible using the finite element method. In actual field problems hydrodynamic loads due to wave and currents act simultaneously on spar platform and mooring lines. Finite element model has been established to cope up all the dynamic behaviour in support of precise computation (Baušys *et al.* 2008; Chow, Li 2010; Mang 2009). In this FE model, the entire structure acts as a continuum. This model can handle all non-linearities, loading and boundary conditions.

The equation of motion has been solved using ABAQUS finite element code. It has the capability of modelling slender and rigid bodies with realistic boundary conditions, including fluid inertia and viscous drag (Jameel 2008). The mooring lines are modelled as three-dimensional tensioned beam elements. It includes the non-linearities due to low strain large deformation and fluctuating pretension. Hybrid beam element is used to model the mooring lines. It is hybrid, because it employs the mixed formulation involving six displacements and axial tension as nodal degrees of freedom. The axial tension maintains the catenary shape of the mooring line. The hybrid beam element is selected for easy convergence, linear or non-linear truss elements can also be considered with associated limitations. The beam element under consideration experiences the wave forces due to Morison's equation. The self-weight and axial tensions are duly incorporated. The force vector consists of the concentrated forces f_x, f_y and f_z and the corresponding moments m_x, m_y and m_z at each node. The three-dimensional stiffness matrix in ABAQUS is capable of including geometric stiffness matrix with elastic stiffness matrix. $[K_G]$ models the large deformation associated with mooring configuration. Instantaneous stiffness matrix with varying axial tension in the modified geometry takes into account the associated non-linearity. The structural damping is simulated by Rayleigh model. Hydrodynamic damping is dominant in case of oscillating slender member surrounded by water.

The spar hull is modelled as an assemblage of rigid beam elements connecting its centre of gravity, riser reaction points and mooring line fair leads. The radius of gyration and the cylinder mass are defined at C.G. The rigid spar platform has been connected to the elastic mooring lines by means of six springs (three for translation and three for rotation). The stiffness of translation springs is very high; whereas the stiffness of rotational springs is very low simulating a hinge connection.

1.4. Solving equation of motion in the time domain

Many schemes have been suggested in the literature for the solution of such equations. Because of the coupled and non-linear nature of the equation of motion, an implicit time-domain analysis is required to obtain the time histories of the response. This approach essentially involves the integration of velocity and acceleration in time domain. In the present work, Newmark-β method is used and the response time histories are obtained in an iterative fashion.

In the implicit iterative solution scheme involving Newmark-β method at a time station T_n, structural velocity, displacement and acceleration are initialized and $[K]$, $[M]$ and $[C]$ matrices and vector $\{F\}$ are determined. The size of time step (Δt), parameters α, δ and integration constants (a_0, a_1, $a_2, \ldots$, a_7) are evaluated. The choice of time interval (Δt) is an essential feature of the solver. Its choice is governed by accuracy and stability criteria. It is also governed either by the rate of load variation in small interval or by the lowest time period of the structure.

An automatic time interval (Δt) incrimination solution scheme is selected. The scheme uses half-step residual control to ensure an accurate dynamic solution. The half-step residual means the equilibrium

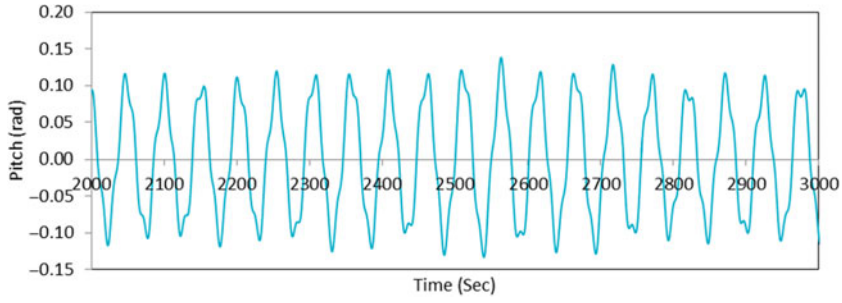

Fig. 12. Pitch time series after 2000 sec. of wave hitting

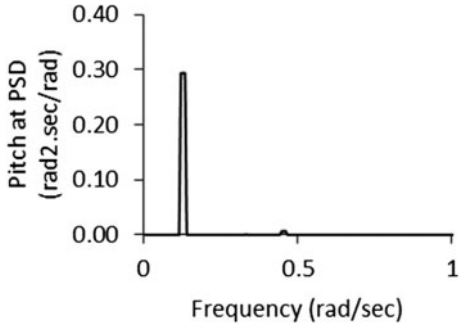

Fig. 13. Pitch response at PSD after 2000 sec. of wave hitting

residual error (out-of-balance forces) halfway through a time increment. For a continuum solution the equilibrium residual should be moderately small related to significant forces in the problem. This half-step residual check is the basis of the adaptive time interval incrimination scheme. If the half-step residual is small, the accuracy of the solution is high and the time step can be increased safely; conversely, if the half-step residual is large, the time step taken in the solution ought to be reduced.

The tolerance limit of convergence is satisfied at every time station. Effective stiffness and effective load vector are then determined. It is to mention that in practical case, surge indicates the wave direction, sway as its orthogonal direction and heave is vertical direction. Roll, pitch and yaw are the direction of rotational responses around surge, sway and heave respectively.

The equations are then solved and at each time step the following parameters are determined:

1. Six components of the structural motion at each node viz. surge, sway, heave, roll, pitch and yaw together with respective velocities and acceleration.
2. Total wave induced forces and moments incorporating structural motion.
3. Stiffness mass and damping matrices.
4. Mooring line tension, nodal displacements and rotations.
5. Sea surface elevation to incorporate variable submergence.

Convergence criteria regulate the number of iterations over the above process and the final values are ascertained at n^{th} time station. The values of the required parameters at n^{th} time station are used to determine the same at $n+1^{\text{th}}$ time station and so on. The time histories for all the above responses at all the nodes and mooring tensions are obtained.

2. Results and discussion

Offshore compliant floating structure like spar platform has been chosen allowing spar mooring coupling in ocean wave at 1018 m deep water. Sea bed size has been chosen as 5000×5000 m^2 for its modelling. The mechanical and geotechnical properties of the spar mooring system under study are given in Table 1.

Table 2 illustrates the hydrodynamic characteristics of sea environment. Mooring tensions are assumed to be equally distributed in all the four mooring lines. The spar hull is expected to behave like a rigid body. When the wave forces act on the entire structure, participation of mooring lines in the overall response is well depicted. The variable boundary conditions due to mooring anchor point are appropriately incorporated. Due to the ideal modelling, the solution is having difficulty in convergence. Responses of spar and mooring lines under regular wave of significant wave height, W_H as 6 m and zero up crossing period, W_P as 14 sec. are plotted at 2000 sec. and 8000 sec.

Through the time-domain analysis adopting step-by-step integration procedure, the excursion time histories are found for sufficient length of time so that the response attains their steady state. The analysis of spar mooring system for deepwater condition has been performed up to a record length of 12,000 sec. This time limit is clearly more than 8000 sec. of wave hitting. To understand the mooring damping and coupling effect, two sets of responses are obtained. The responses in terms of surge, heave, pitch and mooring line tension are plotted between 2000–3000 sec. and 8000–9000 sec. respectively. As the other responses viz. sway, yaw and roll motion of spar hull are trivial, they are not assessed in this study. The statistical characteristics of the spar responses are also determined taking these time lengths of 2000–3000 sec. and 8000–9000 sec. duration. Detail evaluation obviously explains the spar mooring system

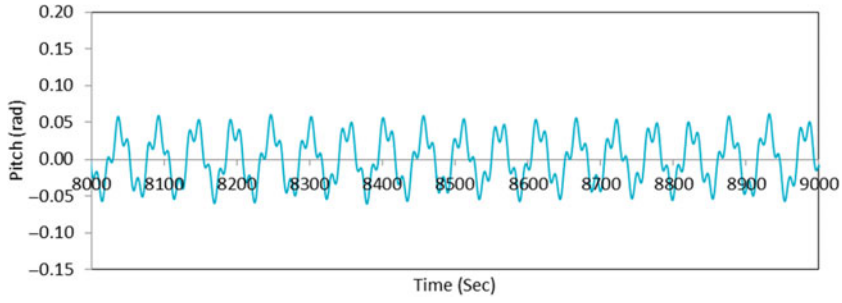

Fig. 14. Pitch time series after 8000 sec. of wave hitting

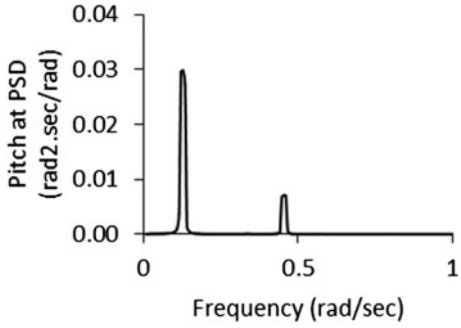

Fig. 15. Pitch response at PSD after 8000 sec. of wave hitting

responses due to coupled analysis after approximately 2000 sec. and 8000 sec. of storm.

2.1. Validation of present coupled integrated model

Integrated coupled analysis of spar mooring system has been performed for 1018 m water depth. The characteristics of spar platform and environmental loading are shown in Table 1 as the well-established published result presented at Chen *et al.* (2001). The static analysis results and natural frequencies obtained by the present study are compared with the existing literature of Chen *et al.* (2001) (Fig. 3).

Chen *et al.* (2001) reported the variation of net tension in four mooring lines at the fair lead position, varying against various static off-sets in surge direction. The responses deals with the regular wave loading for the deepwater condition having water depth 1018 m. Figure 3 shows the same variation of tension versus the spar off-set for 1018 m water depth at range 0–10 m. Later on it shows difference of 6.5% almost equally with Chen *et al.* (2001) for all the off-sets ranging after 10–25 m. However, the trend of the results is quite matching. The variation in the numerical values of net tension is mainly due to the basic difference in mathematical model. The present study takes into account, the actual integrated coupling of entire structure by finite element assembly considering all major non-linearities, while Chen *et al.* (2001) did it differently. The values obtained by the present study closely match with the study carried out by Chen *et al.* (2001). It shows the validity of the coupled mathematical model. The boundary conditions are appropriately implemented for the required state of equilibrium.

Free vibration analysis of spar platform is also carried out. Lanczos method has been used to obtain the natural frequencies and corresponding mode shapes. Table 3 shows the comparison of natural time periods between Chen *et al.* (2001) and the present study. The natural periods obtained by Chen *et al.* (2001) are 322.5, 26.2 and 54.6 sec. in surge, heave and pitch, respectively. The natural periods obtained by the present simulation are close to the experimentally measured values as shown in the Table 4. The difference is marginal in surge but significant in heave and pitch. It may be due to difference in basic models. However, both values seem to be of the same order.

2.2. Response of spar platform after 2000 sec. and 8000 sec.

The coupled form of structural modelling is idealised appropriately. It gives true behaviour of spar mooring system. This approach yields dynamic equilibrium between the forces acting on the spar and the mooring line at every time station. The computational efforts required for the coupled analysis considering a complete model including all mooring lines are substantial. The ability for more accurate prediction of platform motions by coupled analysis approach may consequently contribute to a smaller and comparatively, less expensive spar mooring system and hence, a lighter spar platform through a lessening in payload requirements. The results are shown in Figures 4–23 (Figs 4–7 for surge, Figs 8–11 for heave, Figs 12–15 for pitch and Figs 16–23 for mooring line tension). Both the time series and corresponding power spectral density are presented in these figures. Statistical analyses in terms of maxima, minima, mean and standard deviation are given in Tables 1 and 4 for 2000 sec. and 8000 sec. of wave loading, respectively.

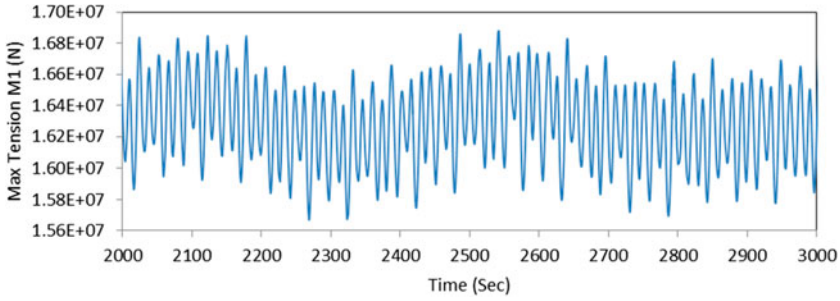

Fig. 16. Maximum tension time series of mooring line 1 after 2000 sec. of wave hitting

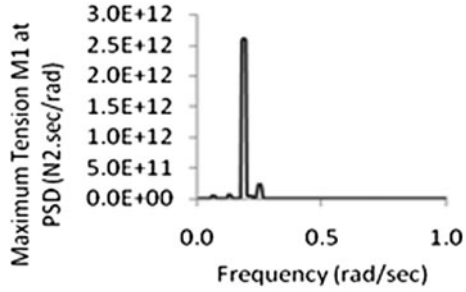

Fig. 17. Maximum tension at mooring line 1 at PSD after 2000 sec. of wave hitting

Surge response

The time series of surge response after 2000 sec. of wave loading at the deck level is shown in Figure 2. The peak of surge response ranges from +16.461 m to −4.105 m (Table 4). The nature of surge at the deck level is predominantly periodic as shown in Figure 4. This is why a single dominant peak occurs in surge response at pitching frequency (Fig. 5). The pitch motion (Fig. 12) occurs simultaneously with surge and attracts significant wave energy close to the pitch frequency. Surge response requires huge energy input because of large inertia and hence do not get excited. However, pitching motion occurring with surge gets excited easily. The surge response at the deck level is mainly dominated by the pitching motion of the hull with insignificant excitation of surge mode. It is mainly due to coupling of surge and pitch. The power spectral density as shown in Figure 5 shows the participation of two frequencies. The small oscillation of the harmonic response occurs at a frequency of 0.465 rad/sec. This is because of the natural frequency. There is no evidence of any significant participation of other frequencies. Effect of non-linearity is not very strong on surge response.

The time series of surge after 8000 sec. of storm is showing a typical regular behaviour as shown in Figure 6. The platform oscillates in regular fashion with maximum and minimum value of 8.143 and 8.342 m. The mean value of surge is given by 0.412 m, whereas the standard deviation of this distribution is found to be 4.913. On comparison of statistics with the surge response in regular wave (Table 5), the above trend is established. The surge time series power spectral density (PSD) at 8000 sec. plus time state shows two distinct peaks (Fig. 7) at 0.130 rad/sec. and 0.461 rad/sec. These peaks correspond to natural frequencies of surge and pitch respectively.

Heave response

The heave response directly influences the mooring tensions and other operations. The heave responses under regular wave are shown in Figure 8. The time series shows the cluster of reversals occurring at varying time intervals. The phenomenon shows the regularity in the behaviour. The statistical Table 4 shows the maximum and minimum responses as 2.453 m and −1.981 m, while the mean value is 0.389. The heave response fluctuates about the mean position oscillating from smaller to larger amplitudes, and repeating the same trend onwards all through the time series as shown in the Figure 8. The fluctuations gradually increase from narrow to broad by 30%. Reaching the peak, it gradually reduces by 30%.

PSD of heave response shows a prominent peak at 0.243 rad/sec. which is close to the natural frequency of heave, while other peaks (Fig. 9) have very small energy content. Such peaks may, however, attract more energy at some other sea state occurring in that region. The response is periodic in nature with superimposed ripples. The local fluctuations near the peaks in the time series have small participation in the response. It is clearly identified that after 8000 sec. of wave striking the maximum heave response in presence of regular wave reduces by approximately 50%. It is because of the static off-set of the hull and mooring behaviour. The heave time series in Figure 10 shows the beating phenomenon. The PSD in Figure 11 shows a solitary peak at natural frequency of heave. But the peak is drastically reduced up to more than 15 times causing a very low magnitude.

Pitch response

Figure 12 shows the pitch response after 2000 sec. time period. The time series shows regular fluctuations ranging from ±0.112 rad. and reducing to small ordinates of ±0.09 rad. at time station 3130 sec. It

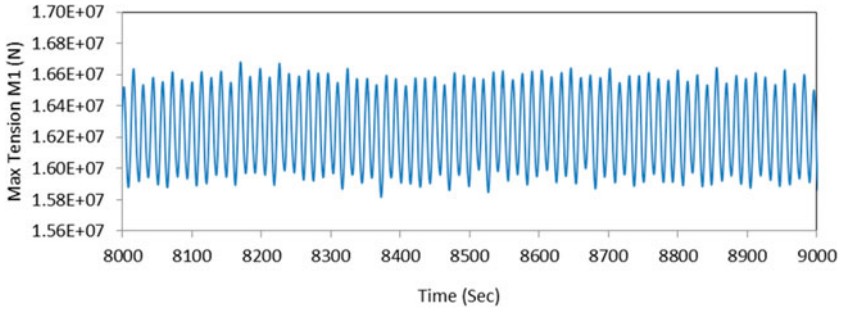

Fig. 18. Maximum tension time series of mooring line 1 after 8000 sec. of wave hitting

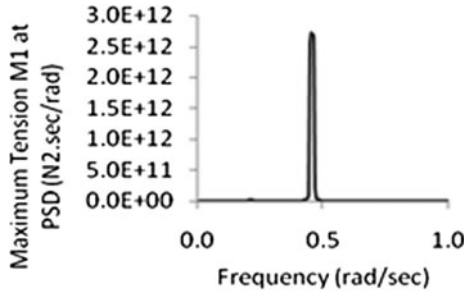

Fig. 19. Maximum tension at mooring line 1 at PSD after 8000 sec. of wave hitting

takes the energy and further increases to ±0.11 rad. The statistical Table 4 that shows the maximum positive and negative pitch values of +0.203 and −0.135 rad. The mean value is almost zero and the standard deviation is 0.079 radians. The mean value of zero shows its regular oscillations about the mean position. The significant value of pitch response leads to a significant surge at deck level. It is coupled with the surge of rigid hull which otherwise is of small magnitude, but gets enhanced due to pitch input. This is why the surge time series at deck level shows maximum peak at pitch frequency (Fig. 5). Like surge response pitch, time series also shows similar behaviour. The periodic response oscillates at frequency of 0.168 rad/sec. about the mean position. It is the wave frequency response as the pitch drives its force from the wave. The frequency of 0.427 rad/sec. is quite close to the natural frequency of pitch response. However, the participation at low frequency is very small.

The pitch response at time state 8000 sec. plus gets significantly modified in comparison to the case with 2000 sec. wave hitting. Figure 14 shows the pitch time series under regular wave after 8000 sec. of storm. Pitching motion is regularly distributed about the mean position. Maximum and minimum values of pitch responses are reduced three times in comparison to the case with 2000 sec. time state. The reason is the damping of pitching motion due to regular wave on spar and mooring system. However, the regularity is more severe here. The PSD of pitch time series as shown in Figure 15 confirms the regular behaviour. The first peak occurs at 0.126 rad/sec. which is close to the pitch natural frequency, while another peak occurs at 0.458 rad/sec. which is the dominant wave loading. The energy content of PSD is, however, significantly small in comparison to that at 2000 sec. time state (Fig. 13). The reduction ranges to 10 times. It is mainly due to the damping of the pitch motion.

Mooring line tension response

The response of mooring lines plays an important role in the coupled dynamic analysis of the spar platform. Mooring lines are physically linked with the spar hull at the fairlead and pinned at the seabed in the finite element model. The regular wave loads simultaneously act on the hull and mooring lines. The analysis of this structure yields the coupled response in true sense.

The designed pretension in each mooring line of the present problem is 1.625E+07 N (Table 1). Mooring line 1 shows the regular behaviour of tension after 2000 sec. of storm (Fig. 16). The PSD of the tension time histories are shown in Figure 17. There are several peaks shown but the maxima occur approximately at 0.18 rad/sec. which is close to the natural frequency of heave. It is expected that heave will significantly influence the mooring tension response. A small peak also occurs, exciting the low frequency surge response. Surge response also causes increase in tension. Other peaks occur at 0.22–0.26 rad/sec. are small, but may get excited under other sea states. The statistics shows the maximum and minimum values as 1.6821E+07 N and 1.5924E+07 N, respectively in mooring line 1 (Table 4). The tension time series of mooring line 3 (Fig. 20) is also regular in nature. It is important from fatigue view point. However, there are slight fluctuations in magnitude. The PSD of time series shows a governed peak at 0.17 rad/sec. (Fig. 21), which is close to the heave natural frequency.

Mooring lines 1 and 3 are positioned in the direction of wave propagation. Mooring line 1 experiences the maximum tension to support surge in the forward direction, while mooring line 3 slackens resulting in the reduction of pretension. Figures 15 and 19 show the tension fluctuations, when mooring line 1 stretches and mooring line 3 slackens due to surge response. Tension fluctuation is of complex periodic nature showing minor ripples near the peaks.

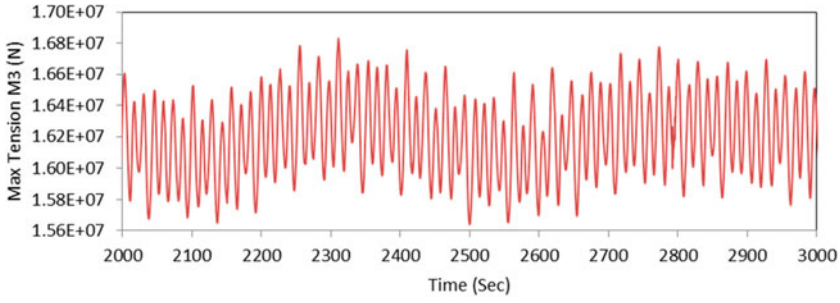

Fig. 20. Maximum tension time series of mooring line 3 after 2000 sec. of wave hitting

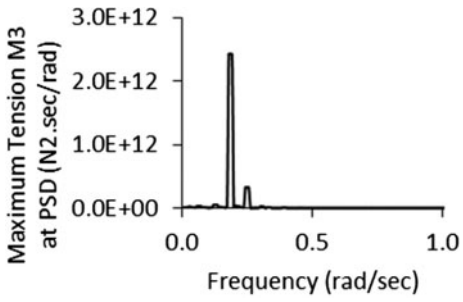

Fig. 21. Maximum tension at mooring line 3 at PSD after 2000 sec. of wave hitting

For both of these mooring lines at the regular wave periodic behaviour is governed. The major peak frequency as shown in PSD matches with the same.

The slack mooring line 3 remains in catenary shape with the reduction in tension. Figure 20 shows the major peak at the wave frequency. The response also shows a large low-frequency peak (0.258 rad/sec.) close to the natural period of surge as shown in Figure 21. On this low-frequency fluctuation, a periodic oscillation at the frequency close to the wave frequency is superimposed. The low-frequency response in mooring lines 1 and 3 is important as it attracts significant energy. Wave frequency response too is quite substantial and should duly be considered. There are very small peaks at several other frequencies whose magnitude is negligible. However, the presence of such peaks shows the tendency of excitation due to changes in mooring line characteristics and forcing behaviour. The non-linear behaviour may also lead to sub and super harmonic resonance. While designing the mooring lines this behaviour should not be ignored.

The coupled spar mooring system changes when 8000 sec. is considered. It is expected more in case of huge time duration when mooring line is affected with damping. Maximum tension time series in mooring line 1 is shown in Figure 18. Regular oscillations are taking place about the mean value of 1.6329E+07 N. The maximum and minimum values of tensions are 1.6695E+07 N and 1.5834E+07 N, which are less than those at 2000 sec. time, state (Table 1). Fluctuations of the time series are also less in case of 8000 sec. of storm. The PSD (Fig. 19) shows clearly a prominent single peak at 0.469 rad/sec. that is quite different from the 2000 sec. time state condition as earlier. This natural frequency is significantly shifted changed to 2.5 times than that at 2000 sec. wave hitting. The participation of heave in mooring tension is significantly small as compared to that with 2000 sec. time state condition (Fig. 22). It is because of the damping effect being active in heave motion. The surge is also contributing in response but with a small magnitude.

The time series of mooring line 3 under regular wave shows a damped response of regular nature. The statistics for mooring line 3 shows the maxima, minima and mean of 1.6702E+07 N, 1.5816E+07 N and 1.6335+07 N, respectively (Table 5). Whereas, for the case of wave at 2000 sec. plus time state, the maxima, minima and mean are 1.6804E+07 N, 1.5743E+07 N and 1.6298E+07 N, respectively, as shown in Table 4. The response is damped out with no further increment because of lateral position of mooring line 3. The maximum tension shows a single dominant peak (Fig. 23) and not any significant peak like that for 2000 sec. time state. The tension time series of mooring line 3 under regular wave at 8000 sec. plus time state shows the mean value smaller than the pretension. Likewise, the maximum and minimum values are also smaller in comparison to that in case of response at 2000 sec. wave hitting. This behaviour is expected, because of slacking of mooring line 3 at 8000 sec. time state.

Conclusions

In deeper water, spar platform is the most suitable structure for oil and gas exploration. The developed finite element model presents an integrated single model of spar mooring system. This model is capable of handling all the non-linearities, loading and boundary conditions. The spar response gets significantly modified and mean position of oscillations gets shifted after longer time of wave hitting. In regular wave ($W_H = 6$ m, $W_P = 14$ sec.) at 1018 m deep, the surge, heave and pitch responses are predominantly excited respectively. However, the low frequency and wave frequency responses may simultaneously occur

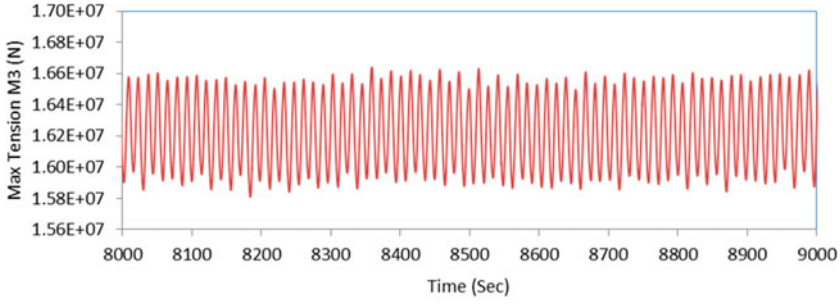

Fig. 22. Maximum tension time series of mooring line 3 after 8000 sec. of wave hitting

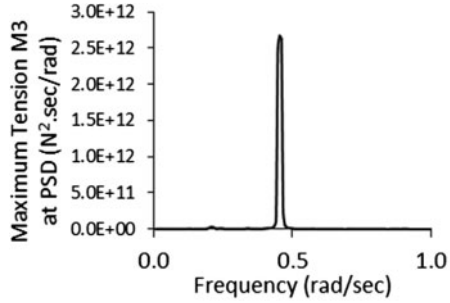

Fig. 23. Maximum tension at mooring line 3 at PSD after 8000 sec. of wave hitting

due to synchronising sea states. The physical coupling of mooring lines at spar fair lead and the variable contact condition at the touch down point near sea bed, model the mooring line dynamics in a realistic fashion. However, the results are convergence sensitive and require large number of iterations, at each time station. The energy contents of PSDs of displacement and rotational motion drastically reduces with time duration. It is mainly due to the damping of mooring line in the integrated coupled spar mooring system. The pitch response is quite sensitive to wave loading. Pitch response is governed by low frequency/natural frequency in both the cases. However, in long storm the magnitude of peaks at low frequency reduces significantly along with little participation of wave frequency response. The mooring tension responses at lower duration show the participation of higher modes near wave frequency apart from exciting an appreciable low-frequency response. At long duration, the response is observed to be predominant only at heave frequency.

Acknowledgements

The authors would like to gratefully acknowledge University of Malaya (UM), for the constant support and the Grant RG093-10AET provided to fund the research work.

References

ABAQUS 6.9.1. 2006. *ABAQUS documentation version 6.6*. Karlson & Sorensen, Inc.

Baušys, R.; Dundulis, G.; Kačianauskas, R.; Markauskas, D.; Rimkevičius, S.; Stupak, E.; Stupak, S.; Šliaupa, S. 2008. Sensitivity of dynamic behaviour of the FE model: case study for the Ignalina NPP reactor building, *Journal of Civil Engineering and Management* 14(2): 121–129. http://dx.doi.org/10.3846/1392-3730.2008.14.7

Chaudhury, G. 2001. A new method for coupled dynamic analysis of platforms, in *Proc. of the 11th International Offshore and Polar Engineering Conference*, 17–22 June, 2001, Stavanger, Norway, 444–448.

Chaudhury, G.; Ho, C.-Y. 2000. Coupled dynamic analysis of platforms, risers, and moorings, in *Proc. of the Offshore Technology Conference*, 1–4 May, 2000, Houston, TX, USA, 8 p.

Chen, X.; Ding, Y.; Zhang, J.; Liagre, P.; Niedzwecki, J.; Teigen, P. 2006. Coupled dynamic analysis of a mini TLP: comparison with measurements, *Ocean Engineering* 33(1): 93–117. http://dx.doi.org/10.1016/j.oceaneng.2005.02.013

Chen, X.; Zhang, J., 1999. Coupled time-domain analysis of the response of a spar and its mooring system, in *Proc. of the 9th International Offshore Polar Engineering Conference (ISOPE)*, 30 May–4 June, 1999, Brest, France, 293–300.

Chen, X.; Zhang, J.; Ma, W. 2001. On dynamic coupling effects between a spar and its mooring lines, *Ocean Engineering* 28(7): 863–887. http://dx.doi.org/10.1016/S0029-8018(00)00026-3

Chow, C. L.; Li, J. 2010. An analytical model on static smoke exhaust in Atria, *Journal of Civil Engineering and Management* 16(3): 372–381. http://dx.doi.org/10.3846/jcem.2010.42

Colby, C.; Sodahl, N.; Katla, E.; Okkenhaug, S. 2000. Coupling effects for a deepwater spar, in *Proc. of the Offshore Technology Conference*, 1–4 May, 2000, Houston, TX, USA, 7 p.

Culla, A.; Carcaterra, A. 2007. Statistical moments predictions for a moored floating body oscillating in random waves, *Journal of Sound and Vibration* 308(1–2): 44–66. http://dx.doi.org/10.1016/j.jsv.2007.07.018

Ding, Y.; Gilbert, R. B.; Purath, B. T.; Dangyach, S.; Zhang, J.; Choi, Y. J. 2005. Reliability of mooring systems for a spar, in *Proc. of the 24th International Conference on Offshore Mechanics and Artic Engineering*, 2005, Halkidiki, Greece, Paper no. 67290.

Ding, Y.; Kim, M.; Chen, X.; Zhang, J. 2003. A numerical code (COUPLE6D) for coupled dynamic analysis of moored offshore structures, in *Proc. of the International Symposium on Deepwater Mooring Systems*, 2003, Houston, TX, USA, 168–182.

Garrett, D. L. 2005. Coupled analysis of floating production systems, *Ocean Engineering* 32(7): 802–816. http://dx.doi.org/10.1016/j.oceaneng.2004.10.010

Grigorenko, A.; Yaremchenko, S. 2009. Investigation of static and dynamic behavior of anisotropic inhomogeneous shallow shells by spline approximation method, *Journal of Civil Engineering and Management* 15(1): 87–93. http://dx.doi.org/10.3846/1392-3730.2009.15.87-93

Gupta, H.; Finn, L.; Weaver, T. 2000. Effects of spar coupled analysis, in *Proc. of the Offshore Technology Conference*, 1–4 May, Houston, TX, USA, 10 p.

Halkyard, J. E. 1996. Status of spar platforms for deepwater production systems, in *Proc. of the 6th International Offshore and Polar Engineering Conference*, 26–31 May, 1996, Los Angeles, CA, USA, Vol 1, 262–272.

Hillis, A. J.; Courtney, C. R. P. 2011. Structural health monitoring of fixed offshore structures using the bicoherence function of ambient vibration measurements, *Journal of Sound and Vibration* 330(6): 1141–1152. http://dx.doi.org/10.1016/j.jsv.2010.09.019

Islam, A. B. M. S.; Jameel, M.; Jumaat, M. Z. 2011a. Effect of time elapse after wave hitting on coupled spar platform, *International Journal of the Physical Sciences* 6(11): 2671–2680.

Islam, A. B. M. S.; Jameel, M.; Jumaat, M. Z.; Shirazi, S. M. 2011b. Spar platform at deep water region in Malaysian sea, *International Journal of the Physical Sciences* 6(30): 6872–6881.

Islam, A. B. M. S.; Jameel, M.; Jumaat, M. Z. 2012. Oil and gas energy potential at Malaysian sea bed and spar platform for deep water installation, *International Journal of Green Energy* 9(2): 111–120. http://dx.doi.org/10.1080/15435075.2011.621493

Jameel, M. 2008. *Non-linear dynamic analysis and reliability assessment of deepwater floating structure*. PhD Dissertation. Indian Institute of Technology, Delhi, India.

Jameel, M.; Ahmad, S. 2011. Fatigue reliability assessment of coupled spar-mooring system, in *Proc. of the 30th International Conference on Ocean, Offshore and Arctic Engineering, Vol. 2. Structures, Safety and Reliability*, 19–24 June, 2011, Rotterdam, Netherlands, 497–505.

Jameel, M.; Ahmad, S.; Islam, A. B. M. S.; Jumaat, M. Z. 2011. Nonlinear analysis of fully coupled integrated spar-mooring line system, in *Proc. of the 21st International Offshore and Polar Engineering Conference*, 19–24 June, Maui, Hawaii, USA, 198–205.

Kim, M.; Lee, J. H. 2011. Study on nonlinear pavement responses of low volume roadways subject to multiple wheel loads, *Journal of Civil Engineering and Management* 17(1): 45–54. http://dx.doi.org/10.3846/13923730.2011.554012

Kim, M. H.; Koo, B. J.; Mercier, R. M.; Ward, E. G. 2005. Vessel/mooring/riser coupled dynamic analysis of a turret-moored FPSO compared with OTRC experiment, *Ocean Engineering* 32(14–15): 1780–1802. http://dx.doi.org/10.1016/j.oceaneng.2004.12.013

Kim, M. H.; Ran, Z.; Zheng, W. 2001a. Hull/mooring coupled dynamic analysis of a truss spar in time domain, *International Journal of Offshore and Polar Engineering* 11(1): 42–54.

Kim, M. H.; Ward, E. G.; Harnig, R. 2001b. Comparison of numerical models for the capability of Hull/Mooring/Riser coupled dynamic analysis for spars and TLPs in deep and ultra deep water, in *Proc. of the 11th Offshore and Polar Engineering Conference*, 17–22 June, 2001, Stravanger, Norway, 474–479.

Koo, B. J.; Kim, M. H.; Randall, R. E. 2004. The effect of nonlinear multi-contact coupling with gap between risers and guide frames on global spar motion analysis, *Ocean Engineering* 31(11–12): 1469–1502. http://dx.doi.org/10.1016/j.oceaneng.2004.01.002

Low, Y. M. 2008. Prediction of extreme responses of floating structures using a hybrid time/frequency domain coupled analysis approach, *Ocean Engineering* 35(14–15): 1416–1428. http://dx.doi.org/10.1016/j.oceaneng.2008.07.006

Low, Y. M.; Langley, R. S. 2008. A hybrid time/frequency domain approach for efficient coupled analysis of vessel/mooring/riser dynamics, *Ocean Engineering* 35(5–6): 433–446. http://dx.doi.org/10.1016/j.oceaneng.2008.01.001

Luo, M.; Zhu, W. Q. 2006. Nonlinear stochastic optimal control of offshore platforms under wave loading, *Journal of Sound and Vibration* 296(4–5): 734–745. http://dx.doi.org/10.1016/j.jsv.2006.01.071

Ma, Q. W.; Patel, M. H. 2001. On the non-linear forces acting on a floating spar platform in ocean waves, *Applied Ocean Research* 23(1): 29–40. http://dx.doi.org/10.1016/S0141-1187(00)00025-0

Ma, H.; Tang, G.-Y.; Hu, W. 2009. Feedforward and feedback optimal control with memory for offshore platforms under irregular wave forces, *Journal of Sound and Vibration* 328(4–5): 369–381. http://dx.doi.org/10.1016/j.jsv.2009.08.025

Mang, H. 2009. On contemporary computational mechanics, *Journal of Civil Engineering and Management* 15(1): 113–128. http://dx.doi.org/10.3846/1392-3730.2009.15.113-128

Mei, C. 2009. Hybrid wave/mode active control of bending vibrations in beams based on the advanced Timoshenko theory, *Journal of Sound and Vibration* 322(1–2): 29–38. http://dx.doi.org/10.1016/j.jsv.2008.11.003

Miedziałowski, C.; Chyży, T.; Krętowska, J. 2007. Numerical model of three-dimensional coupled wall structures, *Journal of Civil Engineering and Management* 13(1): 37–45.

Noorzaei, J.; Abdulrazeg, A. A.; Jaafar, M. S.; Kohnehpooshi, O. 2010. Non-linear analysis of an integral bridge, *Journal of Civil Engineering and Management* 16(3): 387–394. http://dx.doi.org/10.3846/jcem.2010.44

Ormberg, H.; Larsen, K. 1998. Coupled analysis of floater motion and mooring dynamics for a turret-moored ship, *Applied Ocean Research* 20(1–2): 55–67. http://dx.doi.org/10.1016/S0141-1187(98)00012-1

Ran, Z.; Kim, M. H. 1997. Nonlinear coupled responses of a tethered spar platform in waves, *International Journal of Offshore and Polar Engineering* 7(2): 111–118.

Ran, Z.; Kim, M. H.; Niedzwecki, J. M.; Johnson, R. P. 1996. Response of a spar platform in random waves and currents (experiment vs. theory), *International Journal of Offshore and Polar Engineering* 6(1): 27–34.

Ran, Z.; Kim, M. H.; Zheng, W. 1999. Coupled dynamic analysis of a moored spar in random waves and currents (time-domain versus frequency-domain analysis), *Journal of Offshore Mechanics and Arctic Engineering* 121(3): 194–200. http://dx.doi.org/10.1115/1.2829565

Rasiulis, K.; Gurkšnys, K. 2010. Analyses of the stress intensity of the cylindrical tank wall at the place of the geometrical defect, *Journal of Civil Engineering and Management* 16(2): 209–215. http://dx.doi.org/10.3846/jcem.2010.23

Sarkar, I.; Roesset, J. M. 2004. Variability of results of dynamic analysis of spars, in *Proc. of the 14th International Offshore and Polar Engineering Conference*, 23–28 May, 2004, Toulon, France, 650–654.

Shah, A. A.; Umar, A.; Siddiqui, N. A. 2005. A methodology for assessing the reliability of taut and slack mooring systems against instability, *Ocean Engineering* 32(10): 1216–1234. http://dx.doi.org/10.1016/j.oceaneng.2004.11.002

Srinivasan, N.; Chakrabarti, S.; Sundaravadivelu, R.; Kanotra, R. 2008. Hydrodynamics of a SPAR-Type FPSO concept for application as a production platform, in *Proc. of the 27th International Conference on Offshore Mechanics and Arctic Engineering (OMAE2008)*, 12–20 June, 2008, Estoril, Portugal, 93–110.

Tahar, A.; Kim, M. H. 2008. Coupled-dynamic analysis of floating structures with polyester mooring lines, *Ocean Engineering* 35(17–18): 1676–1685. http://dx.doi.org/10.1016/j.oceaneng.2008.09.004

Umar, A.; Datta, T. K. 2003. Nonlinear response of a moored buoy, *Ocean Engineering* 30(13): 1625–1646. http://dx.doi.org/10.1016/S0029-8018(02)00144-0

Vazquez-Hernandez, A. O.; Ellwanger, G. B.; Sagrilo, L. V. S. 2006. Reliability-based comparative study for mooring lines design criteria, *Applied Ocean Research* 28(6): 398–406. http://dx.doi.org/10.1016/j.apor.2007.05.004

Yang, C. K.; Kim, M. H. 2010. Transient effects of tendon disconnection of a TLP by hull–tendon–riser coupled dynamic analysis, *Ocean Engineering* 37(8–9): 667–677. http://dx.doi.org/10.1016/j.oceaneng.2010.01.005

Yung, T.-W.; Sandström, R. E.; Slocum, S. T.; Ding, Z. J.; Lokken, R. T. 2004. Advancement of spar VIV prediction, in *Proc. of Offshore Technology Conference*, 3–6 May, 2004, Houston, TX, USA, 6 p.

Zhang, F.; Yang, J.-M.; Li, R.-P.; Chen, G. 2008. Coupling effects for cell-truss spar platform: comparison of frequency- and time-domain analyses with model tests, *Journal of Hydrodynamics, Ser. B* 20(4): 424–432. http://dx.doi.org/10.1016/S1001-6058(08)60076-1

Zhang, X.; Zou, J. 2002. Coupled effects of risers/supporting guide frames on spar responses, in *Proc. of the 12th International Offshore and Polar Engineering Conference*, 26–31 May, 2002, Kitakyushu, Japan, 231–236.

Mohammed JAMEEL. Received his PhD from Indian Institute of Technology Delhi (IIT Delhi), India. He has successfully completed various sponsored projects involving non-linear analysis of TLPs, spar, FPSO platforms, deep and shallow water mooring lines and risers. The projects were supported by several government and private funding agencies. Presently he is associated with Department of Civil Engineering, University of Malaya, Malaysia. His research interests include non-linear dynamics, earthquake engineering, reliability engineering, offshore structures, artificial neural network and non-linear finite element analysis.

Suhail AHMAD is in the Department of Applied Mechanics, IIT Delhi, India. He earned his academic qualifications from UCS Swansea, UK, IIT Delhi, University of Roorkee, AMU Aligarh, India. He has guided 15 PhD theses. He has more than 100 research papers to his credit. He has made distinguished professional contributions. His research interests include computational mechanics, offshore structures, dynamics, reliability engineering, composites and FEM.

A. B. M. Saiful ISLAM. A PhD candidate and a graduate research assistant at the Department of Civil Engineering, University of Malaya, Malaysia. He is a member of Institution of Engineers, Bangladesh and American Society of Civil Engineers (ASCE). His research interests include offshore structures, non-linear dynamics, seismic protection, base isolation and pounding.

Mohd Zamin JUMAAT. A Professor and Head of the Department of Civil Engineering, University of Malaya, Malaysia. He is a member of Institution of Engineers, Malaysia and a member of the Drafting Code Committee for reinforced concrete structures. His research interests include behaviour of offshore structures, reinforced concrete structural elements, concrete materials, self-consolidating concrete, lightweight concrete and green concrete.